Variable AC Polarity GTAW Fusion Behavior in 5083 Aluminum

Field emission of electrons and dielectric breakdown of surface oxides lead to enhanced weld metal fusion on electrode positive polarity portions of AC current cycles in the variable polarity GTAW process

BY M. A. R. YARMUCH AND B. M. PATCHETT

ABSTRACT. Aluminum alloys are typically welded on AC with the gas tungsten arc welding (GTAW) process. Many power sources have "max penetration" indicated when more than 50% of the AC cycle is spent on electrode negative polarity and "max cleaning" when more than 50% of the cycle is on electrode positive polarity. In the work reported here, weld bead dimensions, notably penetration and bead width, increase with the percentage of electrode positive polarity during the unbalanced square wave AC welding of aluminum alloys with the GTAW process. This is in direct contradiction of conventional assumptions about the role of electrode positive and electrode negative contributions to surface cleaning and fusion behavior during AC welding.

The primary source of the extra base metal melting during electrode positive operation is in the nature of cold cathode field emission of electrons from the base metal. The dielectric breakdown of surface oxide as electrons are emitted also contributes to the increased fusion, but this is not a contributory factor once the weld metal surface is completely clean. Both phenomena require extra energy to be supplied to the cathode, which results in the increased fusion. Earlier works on the gas metal arc welding (GMAW) process confirm this behavior of enhanced melting at the cathode. Positive ion bombardment, thermal convection from the plasma jet, and radiation from the plasma complete the thermal input to the cathode for metal fusion.

Introduction

When discussing the physics of variable polarity arc welding, the simplest case to consider is a DC electric arc with inert gas shielding and a tungsten cathode capable of thermionic emission. The basic schematic is shown in Fig. 1. The arc can be broken up into five distinct regions: anode spot, anode fall space, arc plasma column, cathode fall space, and cathode spot. During electrode negative polarity, electrons flow from the tungsten cathode to the anode (base material) by means of the arc plasma.

The anode spot is the positive electrode that attracts the negative electrons. Collection of electrons at this region leads to intense heating of the anode substrate (discussed in detail below). The small arc region adjacent to the anode spot is termed the anode fall space. This thin layer, estimated to be a micrometer, has a negative space charge and is characterized by a steep voltage gradient that maintains passage of the current. The arc column is electrically neutral plasma consisting of electrons, ions, and neutral atoms or molecules that are in quasi-thermal equilibrium. The voltage gradient, as shown in Fig. 1, is uniform along the length of the column for a given shielding gas. The cathode fall region is the electrical connection between the cathode and the arc column, but is the most poorly understood region of the welding arc. The region is narrow with a voltage gradient steeper than the anode fall region, and there is a net positive space charge. The cathode spot is the location of electron production by thermionic emission. This emission mechanism is only applicable for high melting point and low work-function materials such as carbon, molybdenum, tantalum, or tungsten.

During AC welding, portions of the welding cycle are spent on both electrode negative and positive polarity. The workpiece now produces the electrons during the EP cycle of the waveform. Typical construction materials such as steel and aluminum melt at temperatures much lower than that necessary for thermionic emission. Hence, these materials are nonthermionic and are often termed "cold cathodes." Field emission processes, whereby electrons are removed from the base materials due to the strong localized voltage gradients, are facilitated by an increase in the cathode fall voltage during electrode positive polarity (Ref. 1). The electrode positive cycle during AC welding permits the removal of tenacious surface oxides from aluminum alloys by "cathode sputtering." This phenomenon produces clean weld surfaces and good fusion characteristics in both the gas tungsten arc welding (GTAW) and plasma arc welding (PAW) processes.

Previous arc physics studies suggest that maximum weld depth and fusion volume occur on electrode negative polarity, when electrons stream toward the metal being welded. This is supported by early energy balance work on the GTAW process using DC electrode negative (DCEN) polarity, where approximately 60–80% (Ref. 2) of the heat generated is absorbed at the anode (Refs. 3, 4). This heat input from the arc is primarily from electron condensation plus convection and radiation from the plasma. Radiation and convection heating account for a tiny proportion of the total heat input (Ref. 5). The anode heating due to electron condensation is

$$H_a = I\left(\varnothing + V_a + \frac{3kT}{2e}\right) \quad (1)$$

where H_a = anode heat input, I = arc current, Ø = anode thermionic work function, V_a = anode fall space voltage, and 3kT/2e = electron thermal energy in the high-temperature plasma.

In contrast, the emission processes and thermal characteristics at nonthermionic cathodes, where electrons are emitted primarily by field emission, are not well understood and no similar comprehensive equation exists (Ref. 6). Nonthermionic

M. A. R. YARMUCH is an MSc graduate of Welding Engineering and B. M. PATCHETT is professor emeritus of Welding Engineering at the University of Alberta, Edmonton, Alberta, Canada.

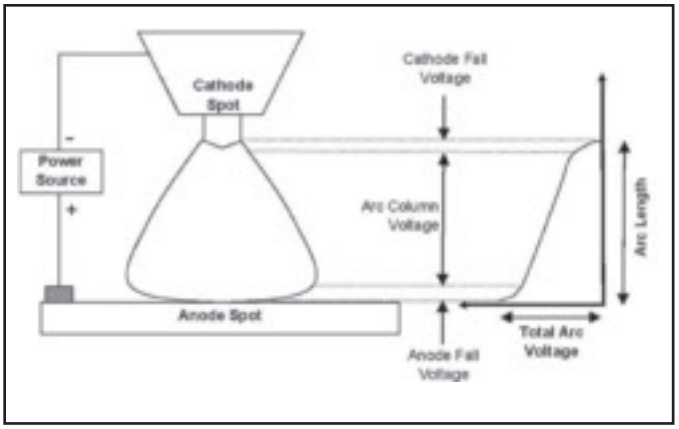

Fig. 1 — Nonconsumable thermionic cathode welding arc: regions of the arc and arc voltage behavior (electrode negative polarity).

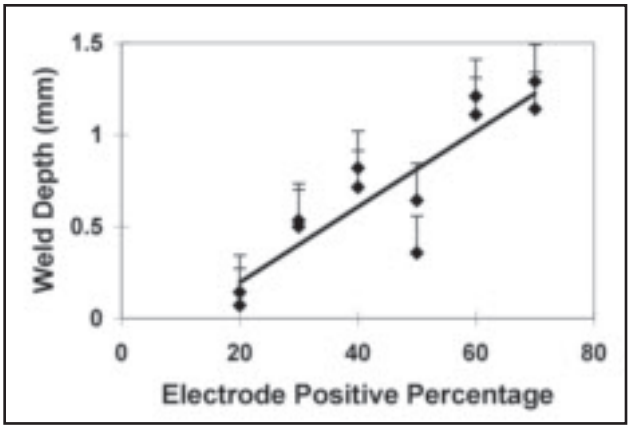

Fig. 2 — Autogenous GTA weld penetration vs. electrode polarity balance — wire-brushed surface.

electrodes emit electrons under large voltage gradients at specific sites, called cathode spots. These spots are highly mobile and often appear at inclusions of lower work function rather than the metallic phase. Aluminum alloys do not have many such inclusions and the electron extraction at an aluminum cathode will normally occur under field emission conditions at many sites on the metal surface.

Previous work on heat transfer in the GTAW and PAW processes has usually been done on copper (Ref. 7) or austenitic stainless steel (Refs. 4, 8) anodes to measure the anode heat input. Little experimental data exist for other metals, especially electrode positive AC effects on aluminum. The low currents and large tungsten electrodes (along with different electrode tip geometry) required for DC electrode positive (DCEP) or AC investigations of heat transfer make duplication of the DCEN experiments for direct comparison very difficult. There has been some investigation of heat inputs to aluminum alloys using AC waveforms, but primarily for the PAW process. Fuerschbach (Ref. 1) found that fusion zone size depended only on net power; no apparent influence of variable polarity on weld fusion dimensions was noted. The same anode/cathode heat balance seen in DC electrode negative GTAW and PAW weld metal fusion is still assumed for AC operation in some publications concerning the processes (Ref. 9).

During the early development of the GTAW process in the 1940s, only balanced 50 or 60 Hz sine wave AC power (50% of each cycle on electrode negative and electrode positive polarity) was available in commercial power sources. Crude forms of square wave AC power became available in the early 1960s, still with balanced waveforms. Power sources including unbalanced waveforms first appeared in the early 1980s with maximum cleaning as 55% electrode positive and maximum penetration as 40% electrode positive. This rather restricted variability in polarity within one AC cycle was due to electronic wave shaping limitations and the need to avoid thermally overloading the tungsten electrodes with excessive percentages of the electrode positive cycle.

General literature on the GTAW process suggests that this characterization of cleaning and penetration is due to "the advantage of surface cleaning associated with conventional AC power and deep penetration obtainable with DCEN power (Refs. 10, 11)." Our experience with these settings in welding process laboratory experiments has been the opposite, i.e., maximum penetration occurs on the maximum cleaning setting, where the majority of each AC cycle is on electrode positive polarity.

Recent developments in solid-state power source design using inverters and advanced wave shape control provide square wave AC at frequencies between 20 and 240 Hz with unbalanced waveforms from 70% electrode positive (maximum cleaning) to 1% electrode positive (maximum penetration). There is also the capacity in some power sources to choose differing levels of current in the positive and negative portions of the current cycle. These enhancements of unbalanced wave capabilities offer significant opportunities to investigate the fundamental effects of AC power on fusion characteristics. The purpose of the work reported in this article was to assess the influence of unbalanced polarity AC waveforms, of constant current magnitude, on the GTAW fusion characteristics of aluminum.

Experimental Program

Autogenous GTA fusion welds were produced on 5083 Al-Mg alloy bars 10 mm thick × 75 mm wide × 300 mm long. Differing types of surface oxide were created by treatments of wire brushing, heat treating (375°C for one hour), and anodizing in nitric acid. All welds used a current of 125 A and a welding speed of 0.8 mm/s (nominal heat input of 1.3 kJ/mm). The 3.2-mm pure tungsten electrode was conditioned at 125 A on a balanced (50% electrode positive) AC cycle for 60 seconds before each run, to ensure that electrode tip geometry was consistent and not a variable in weld bead formation. Arc length was set at 2 mm and the welding-grade argon shielding gas had a constant flow rate of 30 L/min. Electrode positive settings of between 70% and 20% of each AC cycle were assessed using a fixed frequency of 60 Hz. After the pattern of fusion behavior was established for 60 Hz, a set of 50% electrode positive welds using 20, 120, and 240 Hz were made to assess any effects of frequency variations at a fixed electrode positive/negative ratio.

Fusion characteristics were assessed by observing the cleaned surface zone width and by measuring fusion width and depth with a low magnification stereo microscope. Three cross sections were assessed from each weld pass and three welds were made for each experimental condition.

Results

The initial experimental welding was done on aluminum plates that had been degreased and then wire brushed with a stainless steel brush. This ensured both a minimum oxide layer thickness and an even oxide layer thickness. These charac-

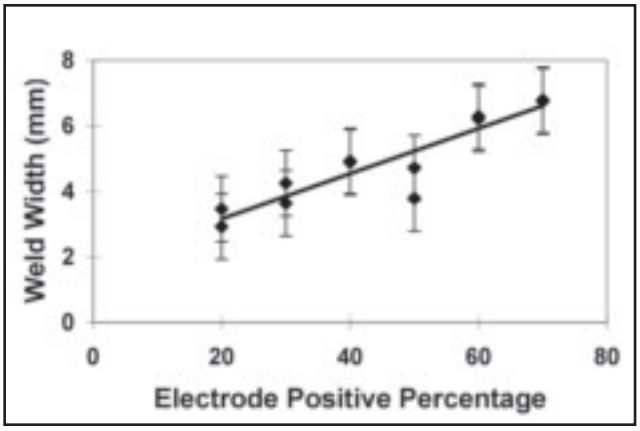

Fig. 3 — Autogenous GTA weld width vs. electrode polarity balance — wire-brushed surface.

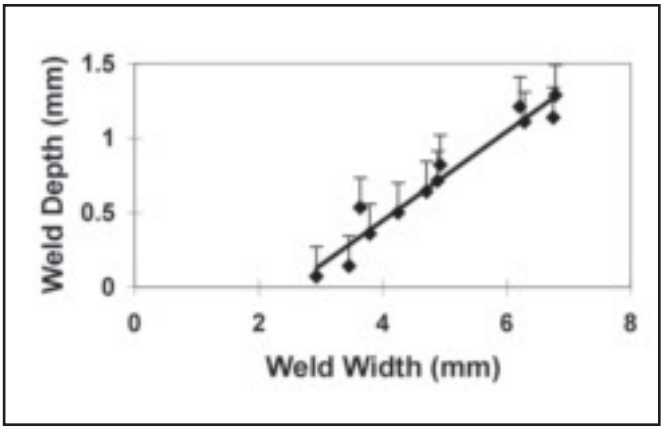

Fig. 4 — Autogenous GTA weld penetration vs. weld width — wire-brushed surface.

teristics were considered important reference states for other welds, where oxide thickness and regularity could be altered via heat treatment and oxide enhancement techniques, e.g., anodizing. Fusion characteristics on the cleaned and wire brushed surface clearly show that increasing the percentage of electrode positive polarity in the AC cycle increases both penetration depth and bead width of an autogenous GTA weld on aluminum, shown in Figs. 2 and 3. As shown in Fig. 4, the penetration increased linearly with the bead width, indicating that the energy for fusion increased with the percentage of electrode positive polarity. Figure 5 shows typical weld cross sections used to measure bead dimensions.

Welds on the heat-treated specimen did not reveal a significant difference in the weld penetration pattern from the wire-brushed specimen. Figure 6 shows the two sets of data for the penetration behavior (error bars are omitted for clarity and are of the same order as reported earlier). The pattern is still consistent with respect to electrode positive polarity in the AC cycle; penetration increased with percent electrode positive in the unbalanced cycle. These results show that a heat-treating cycle (in this case annealing at 375°C) has no measurable effect on arc behavior.

Increasing the oxide layer thickness by anodizing the base metal in nitric acid produced two changes. The weld penetration for a given percent electrode positive in the AC cycle increased from the value for the wire-brushed specimen. These results for the weld depth are shown in Fig. 6 for comparison. Figure 7 shows a similar but lesser result for the weld width. The second difference in the anodized specimens was that the observed sputtered width (not the fusion width) was reduced in comparison with the wire brushed and heat-treated specimens. This suggests that the thicker oxide produced by anodizing is more difficult to disrupt via cathode sputtering. The extra energy used to pull electrons from the aluminum cathode on electrode positive polarity in the presence of a thick oxide layer enhances fusion, rather than reducing it.

The final experiment assessed the effect, if any, of AC frequency on fusion characteristics. Variable frequency AC waveforms have been readily available since the advent of inverter power supplies. The power source used in these experiments was capable of frequency variations between 20 and 240 Hz, which offered a good experimental range around the standard frequency of 60 Hz. The results, shown in Fig. 8, indicate that frequency has no effect on fusion characteristics for a balanced 50% electrode positive AC waveform. It remains to be determined whether or not there is a measurable effect of unbalanced waveforms on fusion behavior at differing frequencies.

Discussion

The results show that maximum fusion width and penetration occurs in GTAW procedures on aluminum with a maximum cleaning (more electrode positive percentage) setting on an unbalanced AC waveform. This phenomenon occurs on cleaned and wire-brushed surfaces with minimum oxide and increases with enhanced oxide thickness developed on anodized specimens. When the GTAW process is on electrode positive polarity, the electrons needed to maintain the majority of the current flow must be extracted from the weld pool. As aluminum is a cold cathode material, the electrons are extracted from mobile cathode spots via field emission. Longer times spent on electrode positive polarity increase the weld penetration via the extra energy input from field emission and increase the weld width via the enhanced area covered by the mobile cathode spots seeking new locations for electron emission.

When up to 70% electrode positive waveforms are used, thicker surface oxides enhance penetration and (to a lesser extent) weld width, shown in Figs. 6 and 7, but restrict sputtered width. Thick oxides produced by anodizing are more difficult to disrupt. This resilience restricts the area of arc impingement and increases the energy density forming the weld pool at a given arc power. This is confirmed by the narrower cleaned zone (not weld width) produced on anodized vs. heat-treated specimens. The cleaned (sputtered) zone is slightly wider than the fused weld width.

Oxides on the surface of the weld metal are disrupted during the electrode positive portion of the AC cycle. The two probable mechanisms, which likely work in concert, are positive ion bombardment (Ref. 12) (primarily from inert gas atoms from the shielding gas) and dielectric breakdown of the oxide during electron extraction from the cathode (Ref. 13). Both phenomena add energy to the cathode and are capable of enhancing the amount of fusion. Oxide disruption is reasonably complete in balanced wave AC operation. In the case of the unbalanced AC wave, increasing the percentage of electrode positive current increases the time spent extracting electrons from aluminum via field emission. The energy required for this process then increases the amount of fusion. Figure 9 summarizes these effects in schematic form.

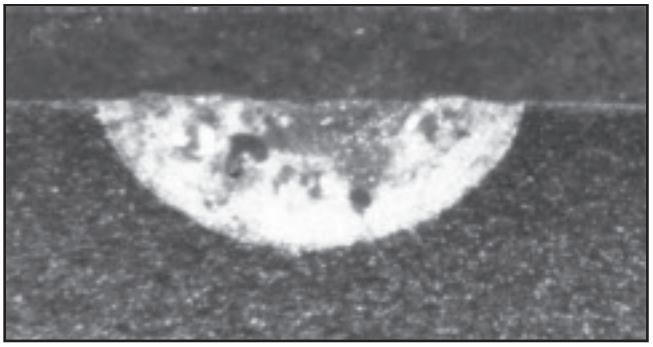

Fig. 5 — Typical cross section of weld zone used for bead measurements.

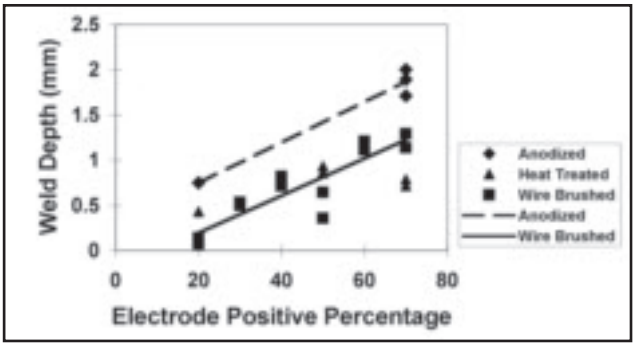

Fig. 6 — Effect of heat treating and anodizing on autogenous weld penetration vs. electrode polarity balance.

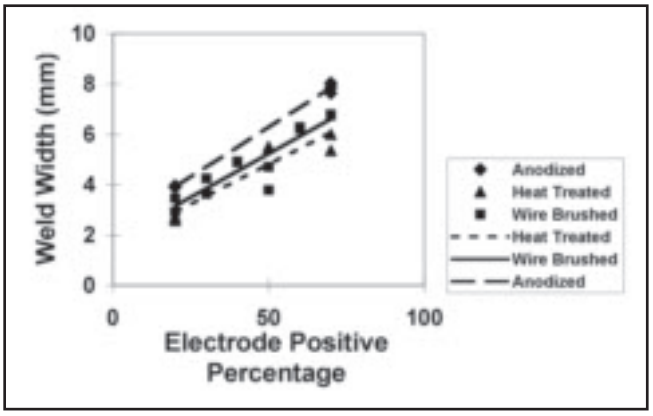

Fig. 7 — Effect of heat treating and anodizing on autogenous weld width vs. electrode polarity balance.

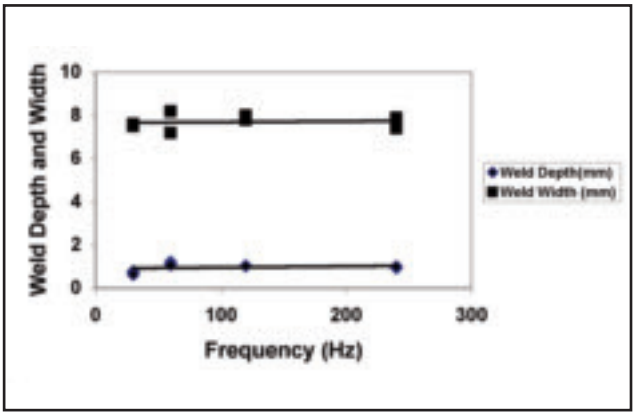

Fig. 8 — Weld metal depth and width vs. AC waveform frequency for a balanced waveform (50% electrode positive).

To some degree, the confusion over the relative melting rates of the anode and cathode in GTAW on AC is caused by the effects of electrode positive polarity on the melting of the tungsten electrode. The tungsten anode is heated by electron condensation and the poor thermal conductivity of tungsten leads to overheating and melting. This effect suggests that the max cleaning mode increases the heat input into the tungsten anode and at the same time reduces the heat input into the weld metal cathode. This is not necessarily the case. When the tungsten is the cathode, thermionic electron emission cools the tungsten as the electrons "evaporate." For nonthermionic emitters, there is an increase in cathode (workpiece) heating due to the absence of the cathode cooling phenomenon during the field emission process. An increase in the cathode fall voltage (Ref. 1) and the corresponding increase in energy required to extract electrons from the cold cathode similarly contribute to the increased workpiece fusion observed in the variable polarity experiments.

The most clearly documented cold cathode effect on cathode heat input is the electrode melting rate in the gas metal arc welding (GMAW) process, which is always higher on electrode negative polarity for cold cathode metals (Refs. 14, 15). The cathode melting rate is up to double the rate for an anode in similar welding conditions. Although some papers assume that the same heat partition exists between anode and cathode for both GTAW and GMAW (Ref. 16), the experimental facts clearly show that the heat input (melting rate) to a GMAW cold cathode is substantially higher than for an anode of similar geometry (Refs. 13, 14). This effect can be reduced through the addition of oxidizing atoms to the shielding gas, for example chlorine in argon, which reduces the energy required to extract electrons from the surface of the cathode (Refs. 17, 18), and therefore reduces the electrode melting rate, or by using emissive coatings on the electrode surface, which provide a similar function (Ref. 13). Electrode melting rates are reduced from bare wire values in both cases. In the absence of such electron emission enhancers, the extra energy required to extract the electrons from the cold cathode metal increases the melting rate.

In the GTAW process, the cold cathode material also experiences the higher heat input, causing the larger weld beads observed here as the percentage of electrode positive time increases. Enhanced oxide thickness, particularly from anodizing, increases the difficulty of extracting electrons, thus further concentrating and increasing heat input.

Pang et al. found that AC welding of aluminum with the plasma arc welding (PAW) process produces welds of superior mechanical and aesthetic quality when compared to DCEN (Ref. 19). Fuerschbach highlighted that a higher percentage of DCEN during variable AC welding with PAW does not translate into greater fusion/penetration, due to the now greater influence of the cold cathode field emission mechanism (Ref. 1). An area of future work would be to completely characterize weld fusion in tungsten arc processes as a function of phase balance

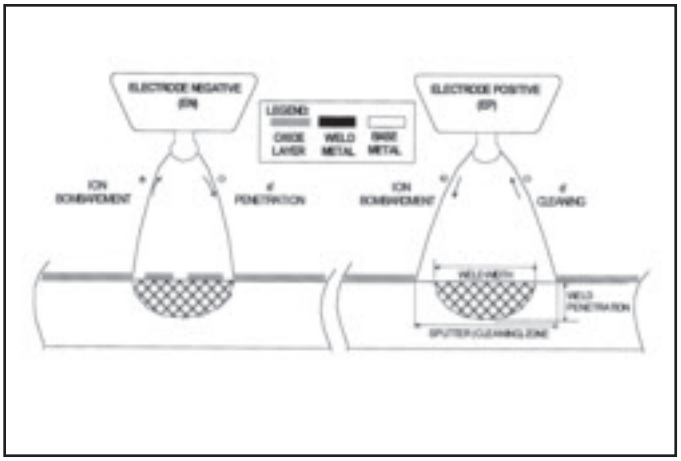

Fig. 9 — Schematic of electron and ion effects in electrode negative and electrode positive GTAW fusion.

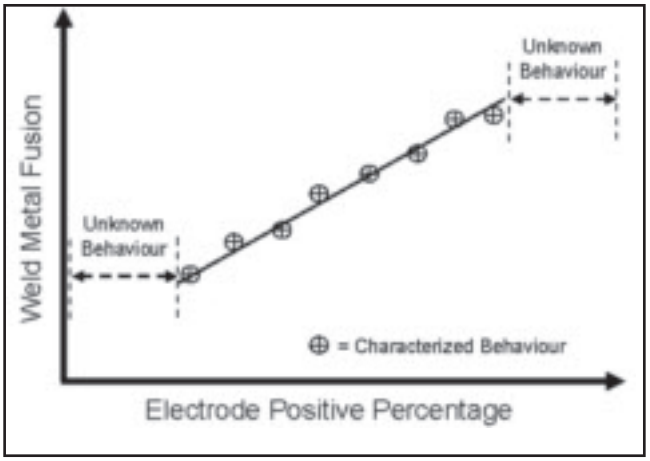

Fig. 10 — Schematic of weld metal fusion behavior as a function of electrode positive percentage during AC welding of aluminum.

(i.e., from 1 to 100% DCEP), and determine the theorized locations of the maximum and minimum weld metal fusion — Fig. 10. This information will further advance the knowledge of welding arc physics, and determine the electron mechanisms that dominate fusion behavior for the entire range of variability polarity welding. A practical effect is possible in the root welding of aluminum pipe, where control of the penetration is critical.

Conclusions

1) Increased weld bead fusion, penetration, and volume occur in autogenous GTAW of 5083 aluminum alloy as the electrode positive polarity (cleaning) portion of the cycle in square wave AC welding increases. This is contrary to conventional expectations and occurs primarily because the field emission characteristics of cold cathode materials increase the energy input to the cathode.

2) Oxidized surface layers enhance fusion volume and penetration. This occurs primarily due to a physical constriction of the sputtered surface area on electrode positive polarity (thus increasing energy density in the weld zone). There may also be a secondary effect in the energy required to extract electrons from the cathode surface via dielectric breakdown of a thicker oxide during electrode positive parts of the AC cycle, which would increase energy input to the cathode (weld pool).

3) Frequency variations of the AC cycle between 20 and 240 Hz apparently do not affect the fusion geometry dimensions, at least for balanced polarity (50% electrode positive) waveforms.

Acknowledgments

The authors wish to thank Clark Bicknell of the Welding Laboratory at the University of Alberta for valuable technical assistance, and students Patricia Cameron, Evan McKnight, and Marcy Wine for assistance in the execution of the experimental program.

References

1. Fuerschbach, P. W. 1998. Cathodic cleaning and heat input in variable polarity plasma arc welding of aluminum. *Welding Journal* 77(2): 76-s.

2. Giedt, W. H., Tallerico, L. N., and Fuerschbach, P. W. 1989. GTA welding efficiency: calorimetric and temperature field measurements. *Welding Journal* 68(1): 28-s.

3. Milner, D. R. et al. 1960. Arc characteristics and their significance in welding. *British Welding Journal* 7(2): 73.

4. Goldman, K. 1963. Electric arcs in argon-heat distribution. *British Welding Journal* 10(7): 343.

5. Fuerschbach, P. W., and Knorovsky, G. A. 1991. A study of melting efficiency in plasma arc and gas tungsten arc welding. *Welding Journal* 70(11): 287-s.

6. Lancaster, J. F. (ed). 1986. *The Physics of Welding*. pp. 169–172. Oxford., Pergamon.

7. Jackson, C. E. 1960. The science of arc welding. *Welding Journal* 39(4): 129-s, 39(6): 177-s.

8. Lu, M., and Ku, S. 1988. Power and current distributions in gas tungsten arcs. *Welding Journal* 67(2): 29-s.

9. Martinez, L. F., Matlock, C., Marques, R. E., McClure, J. C., and Nunes Jr., A. C. 1994. Effect of weld gases on melt zone size in VPPA welding of Al 2219. *Welding Journal* 73(10): 51.

10. American Welding Society. 1996. *Welding Handbook,* W. R. Oates, ed., Eighth edition, Vol. 3, pp. 37, 38.

11. American Welding Society. 1991. *Welding Handbook*, R. L. O'Brien, ed., Eighth edition, Vol. 2, p. 86.

12. Lancaster, J. F. 1984. *The Physics of Weldin*g. Pergamon Press, Oxford, p. 123.

13. Guile, A. E. 1979. Processes at arc cathode roots on non-refractory arc cathodes with relatively thick oxide films. *Proceedings of International Conference on Arc Physics and Weld Pool Behavior.* The Welding Institute, London,UK, p. 79.

14. Lesnewich, A. 1955. Electrode activation for inert-gas-shielded metal-arc welding. *Welding Journal* 34(12): 1167.

15. Lesnewich, A. 1958. Control of melting rate and metal transfer in GMAW. *Welding Journal* 37(8): 343-s, 37(9): 418-s.

16. Quigley, M. B. C. 1977. Physics of the welding arc. *Welding & Metal Fabrication* 45(12): 619.

17. Bicknell, A. C., and Patchett, B. M. 1985. GMA welding of aluminum with argon/freon shielding gas mixtures. *Welding Journal* 64(5): 21.

18. Patchett, B. M. 1978. MIG welding of aluminium with an argon-chlorine mixture. *Metal Construction* 10(10): 484.

19. Pang, Q., Pang, T., McClure, J. C., and Nunes, A. C. 1994 Workpiece cleaning during variable polarity plasma arc welding of aluminum. *Journal of Engineering for Industry – Transactions of the ASME*, 116, (11): 463.